



# Numerical schemes for the simulation of seismic wave propagation in frequency domain

M. Bonnasse-Gahot<sup>1,2</sup>, H. Calandra<sup>3</sup>, J. Diaz<sup>1</sup> and S. Lanteri<sup>2</sup>

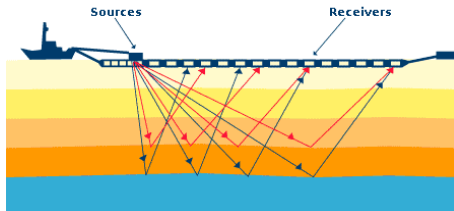
<sup>1</sup> INRIA Bordeaux-Sud-Ouest, team-project *Magique 3D*

<sup>2</sup> INRIA Sophia-Antipolis-Méditerranée, team-project *Nachos*

<sup>3</sup> TOTAL Exploration-Production

# Motivation

## Examples of seismic applications



# Motivation

## Imaging method : the full wave inversion

- ▶ Iterative procedure using the wavefield in order to obtain quantitative **high resolution** images of the subsurface physical parameters

# Motivation

Imaging method : the full wave inversion

- ▶ Iterative procedure using the wavefield in order to obtain quantitative **high resolution** images of the subsurface physical parameters

Seismic imaging : time-domain or harmonic-domain ?

- ▶ Time-domain : **imaging condition complicated** but **low computational cost**
- ▶ Harmonic-domain : **imaging condition simple** but **huge computational cost**

# Motivation

Imaging method : the full wave inversion

- ▶ Iterative procedure using the wavefield in order to obtain quantitative **high resolution** images of the subsurface physical parameters

Seismic imaging : time-domain or harmonic-domain ?

- ▶ Time-domain : **imaging condition complicated** but **low computational cost**
- ▶ Harmonic-domain : **imaging condition simple** but **huge computational cost**

Forward problem of the inversion process

- ▶ Elastic wave propagation in harmonic domain : **Helmholtz equation**
- ▶ Reduction of the size of the linear system

# Motivation

Seismic imaging in heterogeneous complex media

- ▶ Complex topography
- ▶ High heterogeneities

# Motivation

Seismic imaging in heterogeneous complex media

- ▶ Complex topography
- ▶ High heterogeneities

Use of unstructured meshes with FE methods

# Motivation

Seismic imaging in heterogeneous complex media

- ▶ Complex topography
- ▶ High heterogeneities

Use of unstructured meshes with FE methods

DG method

- ▶ Flexible choice of interpolation orders ( $p$  – adaptativity)
- ▶ Highly parallelizable method
- ▶ Increased computational cost as compared to classical FEM

# Motivation

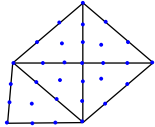
Seismic imaging in heterogeneous complex media

- ▶ Complex topography
- ▶ High heterogeneities

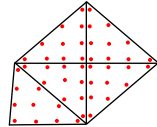
Use of unstructured meshes with FE methods

DG method

- ▶ Flexible choice of interpolation orders ( $p$  – adaptativity)
- ▶ Highly parallelizable method
- ▶ Increased computational cost as compared to classical FEM



DOF of classical FEM



DOF of DGM

# Motivation

## Objective of this work

- ▶ Development of an hybridizable DG (HDG) method
- ▶ Comparison with a reference method : a standard nodal DG method

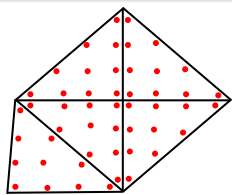


FIGURE : Degrees of freedom of DGM

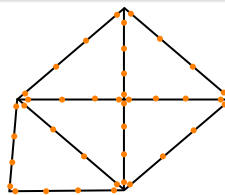


FIGURE : Degrees of freedom of HDGM

# HDG methods

## HDG methods

- ▶ **B. Cockburn, J. Gopalakrishnan, R. Lazarov** *Unified hybridization of discontinuous Galerkin, mixed and continuous Galerkin methods for second order elliptic problems*, SIAM Journal on Numerical Analysis, Vol. 47 (2009)
- ▶ **S. Lanteri, L. Li, R. Perrussel**, *Numerical investigation of a high order hybridizable discontinuous Galerkin method for 2d time-harmonic Maxwell's equations*, COMPEL, Vol. 32 (2013) (time-harmonic domain)
- ▶ **N.C. Nguyen, J. Peraire, B. Cockburn**, *High-order implicit hybridizable discontinuous Galerkin methods for acoustics and elastodynamics*, J. of Comput. Physics, Vol. 230 (2011) (time domain for seismic applications)

# Contents

2D Helmholtz elastic equations

Notations and definitions

Hybridizable Discontinuous Galerkin method

Numerical results

Conclusions-Perspectives

# 2D Helmholtz elastic equations

## First order formulation of Helmholtz wave equations

$\mathbf{x} = (x, y) \in \Omega \subset \mathbb{R}^2$ ,

$$\begin{cases} i\omega \rho(\mathbf{x}) \mathbf{v}(\mathbf{x}) = \nabla \cdot \underline{\sigma}(\mathbf{x}) + f_s(\mathbf{x}) \\ i\omega \underline{\sigma}(\mathbf{x}) = \underline{\underline{C}}(\mathbf{x}) \underline{\underline{\varepsilon}}(\mathbf{v}(\mathbf{x})) \end{cases}$$

- ▶ Free surface condition :  $\underline{\underline{\sigma}} \mathbf{n} = 0$  on  $\Gamma_f$
- ▶ Absorbing boundary condition :  $\underline{\underline{\sigma}} \mathbf{n} = \nu_p(\mathbf{v} \cdot \mathbf{n}) \mathbf{n} + \nu_s(\mathbf{v} \cdot \mathbf{t}) \mathbf{t}$  on  $\Gamma_a$

- ▶  $\mathbf{v}$  : velocity vector
- ▶  $\underline{\sigma}$  : stress tensor
- ▶  $\underline{\underline{\varepsilon}}$  : strain tensor

# 2D Helmholtz elastic equations

## First order formulation of Helmholtz wave equations

$$\mathbf{x} = (x, y) \in \Omega \subset \mathbb{R}^2,$$

$$\begin{cases} i\omega \rho(\mathbf{x}) \mathbf{v}(\mathbf{x}) = \nabla \cdot \underline{\underline{\sigma}}(\mathbf{x}) + \mathbf{f}_s(\mathbf{x}) \\ i\omega \underline{\underline{\sigma}}(\mathbf{x}) = \underline{\underline{C}}(\mathbf{x}) \underline{\underline{\varepsilon}}(\mathbf{v}(\mathbf{x})) \end{cases}$$

- ▶ Free surface condition :  $\underline{\underline{\sigma}} \mathbf{n} = 0$  on  $\Gamma_f$
- ▶ Absorbing boundary condition :  $\underline{\underline{\sigma}} \mathbf{n} = v_p(\mathbf{v} \cdot \mathbf{n}) \mathbf{n} + v_s(\mathbf{v} \cdot \mathbf{t}) \mathbf{t}$  on  $\Gamma_a$

- |  |  |
|--|--|
| <ul style="list-style-type: none"> <li>▶ <math>\rho</math> : mass density</li> <li>▶ <math>\underline{\underline{C}}</math> : tensor of elasticity coefficients</li> </ul> | <ul style="list-style-type: none"> <li>▶ <math>v_p</math> : P-wave velocity</li> <li>▶ <math>v_s</math> : S-wave velocity</li> <li>▶ <math>f_s</math> : source term, <math>f_s \in L^2(\Omega)</math></li> </ul> |
|--|--|

# Contents

2D Helmholtz elastic equations

Notations and definitions

Hybridizable Discontinuous Galerkin method

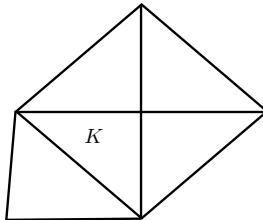
Numerical results

Conclusions-Perspectives

# Notations and definitions

## Notations

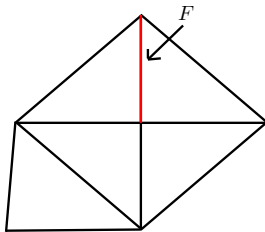
- $\mathcal{T}_h$  mesh of  $\Omega$  composed of triangles  $K$



# Notations and definitions

## Notations

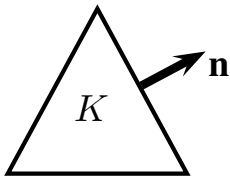
- ▶  $\mathcal{T}_h$  mesh of  $\Omega$  composed of triangles  $K$
- ▶  $\mathcal{F}_h$  set of all faces  $F$  of  $\mathcal{T}_h$



# Notations and definitions

## Notations

- ▶  $\mathcal{T}_h$  mesh of  $\Omega$  composed of triangles  $K$
- ▶  $\mathcal{F}_h$  set of all faces  $F$  of  $\mathcal{T}_h$
- ▶  $\mathbf{n}$  the normal outward vector of an element  $K$



# Notations and definitions

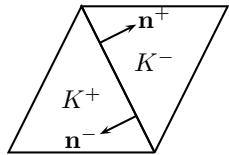
## Definitions

- ▶ Jump  $\llbracket \cdot \rrbracket$  of a vector  $\mathbf{v}$  through  $F$  :

$$\llbracket \mathbf{v} \rrbracket = \mathbf{v}^+ \cdot \mathbf{n}^+ + \mathbf{v}^- \cdot \mathbf{n}^- = \mathbf{v}^+ \cdot \mathbf{n}^+ - \mathbf{v}^- \cdot \mathbf{n}^+$$

- ▶ Jump of a tensor  $\underline{\underline{\sigma}}$  through  $F$  :

$$\llbracket \underline{\underline{\sigma}} \rrbracket = \underline{\underline{\sigma}}^+ \mathbf{n}^+ + \underline{\underline{\sigma}}^- \mathbf{n}^- = \underline{\underline{\sigma}}^+ \mathbf{n}^+ - \underline{\underline{\sigma}}^- \mathbf{n}^+$$



# Contents

2D Helmholtz elastic equations

Notations and definitions

Hybridizable Discontinuous Galerkin method  
Formulation

Numerical results

Conclusions-Perspectives

# HDG formulation of the equations

## Local HDG formulation

$$\left\{ \begin{array}{l} \int_K i\omega \rho^K \mathbf{v}^K \cdot \mathbf{w} + \int_K \underline{\underline{\sigma}}^K : \nabla \mathbf{w} - \int_{\partial K} \hat{\underline{\underline{\sigma}}}^{\partial K} \cdot \mathbf{n} \cdot \mathbf{w} = 0 \\ \int_K i\omega \underline{\underline{\sigma}}^K : \underline{\underline{\xi}} + \int_K \mathbf{v}^K \cdot \nabla \cdot (\underline{\underline{C}}^K \underline{\underline{\xi}}) - \int_{\partial K} \hat{\mathbf{v}}^{\partial K} \cdot \underline{\underline{C}}^K \underline{\underline{\xi}} \cdot \mathbf{n} = 0 \end{array} \right.$$

# HDG formulation of the equations

## Local HDG formulation

$$\begin{cases} \int_K i\omega \rho^K \mathbf{v}^K \cdot \mathbf{w} + \int_K \underline{\underline{\sigma}}^K : \nabla \mathbf{w} - \int_{\partial K} \hat{\underline{\underline{\sigma}}}^{\partial K} \cdot \mathbf{n} \cdot \mathbf{w} = 0 \\ \int_K i\omega \underline{\underline{\sigma}}^K : \underline{\underline{\xi}} + \int_K \mathbf{v}^K \cdot \nabla \cdot (\underline{\underline{C}}^K \underline{\underline{\xi}}) - \int_{\partial K} \hat{\mathbf{v}}^{\partial K} \cdot \underline{\underline{C}}^K \underline{\underline{\xi}} \cdot \mathbf{n} = 0 \end{cases}$$

We define :

$$\begin{aligned} \hat{\mathbf{v}}^F &= \lambda^F, & \forall F \in \mathcal{F}_h, \\ \hat{\underline{\underline{\sigma}}}^{\partial K} \cdot \mathbf{n} &= \underline{\underline{\sigma}}^K \cdot \mathbf{n} - \tau \mathbf{I} (\mathbf{v}^K - \lambda^{\partial K}), & \text{on } \partial K \end{aligned}$$

where  $\tau$  is the stabilization parameter ( $\tau > 0$ )

$\hat{\underline{\underline{\sigma}}}^K$  and  $\hat{\mathbf{v}}^K$  are numerical traces of  $\underline{\underline{\sigma}}^K$  and  $\mathbf{v}^K$  respectively on  $\partial K$

# HDG formulation of the equations

## Local HDG formulation

We replace  $\hat{\mathbf{v}}^K$  and  $(\underline{\hat{\sigma}}^K \cdot \mathbf{n})$  by their definitions into the local equations

$$\left\{ \begin{array}{l} \int_K i\omega \rho^K \mathbf{v}^K \cdot \mathbf{w} + \int_K \underline{\underline{\sigma}}^K : \nabla \mathbf{w} - \int_{\partial K} \underline{\underline{\sigma}}^K \cdot \mathbf{n} \cdot \mathbf{w} \\ \qquad \qquad \qquad + \int_{\partial K} \tau \mathbf{I} (\mathbf{v}^K - \lambda^{\partial K}) \cdot \mathbf{w} = 0 \\ \int_K i\omega \underline{\underline{\sigma}}^K : \underline{\underline{\xi}} + \int_K \mathbf{v}^K \cdot \nabla \cdot (\underline{\underline{C}}^K \underline{\underline{\xi}}) - \int_{\partial K} \lambda^{\partial K} \cdot \underline{\underline{C}}^K \underline{\underline{\xi}} \cdot \mathbf{n} = 0 \end{array} \right.$$

# HDG formulation of the equations

## Local HDG formulation

$$\left\{ \begin{array}{l} \int_K i\omega \rho^K \mathbf{v}^K \cdot \mathbf{w} - \int_K (\nabla \cdot \underline{\underline{\sigma}}^K) \cdot \mathbf{w} + \int_{\partial K} \tau \mathbf{I} (\mathbf{v}^K - \lambda^{\partial K}) \cdot \mathbf{w} = 0 \\ \int_K i\omega \underline{\underline{\sigma}}^K : \underline{\underline{\xi}} + \int_K \mathbf{v}^K \cdot \nabla \cdot (\underline{\underline{C}}^K \underline{\underline{\xi}}) - \int_{\partial K} \lambda^{\partial K} \cdot \underline{\underline{C}}^K \underline{\underline{\xi}} \cdot \mathbf{n} = 0 \end{array} \right.$$

# HDG formulation of the equations

## Transmission condition

In order to determine  $\lambda^K$ , the continuity of the normal component of  $\underline{\hat{\sigma}}^K$  is weakly enforced, rendering this numerical trace conservative :

$$\int_F [\underline{\hat{\sigma}}^K \cdot \mathbf{n}] \cdot \eta = 0$$

# HDG formulation of the equations

## Transmission condition

In order to determine  $\lambda^K$ , the continuity of the normal component of  $\underline{\hat{\sigma}}^K$  is weakly enforced, rendering this numerical trace conservative :

$$\int_F [\underline{\hat{\sigma}}^K \cdot \mathbf{n}] \cdot \eta = 0$$

Replacing  $(\underline{\hat{\sigma}}^K \cdot \mathbf{n})$  and summing over all faces, the transmission condition becomes :

$$\sum_{K \in \mathcal{T}_h} \int_{\partial K} (\underline{\hat{\sigma}}^K \cdot \mathbf{n}) \cdot \eta - \sum_{K \in \mathcal{T}_h} \int_{\partial K} \tau \mathbf{I} (\mathbf{v}^K - \lambda^{\partial K}) \cdot \eta = 0$$

# HDG formulation of the equations

## Global HDG formulation

$$\left\{ \begin{array}{l} \int_K i\omega \rho^K \mathbf{v}^K \cdot \mathbf{w} - \int_K (\nabla \cdot \underline{\underline{\sigma}}^K) \cdot \mathbf{w} + \int_{\partial K} \tau \mathbf{I} (\mathbf{v}^K - \lambda^{\partial K}) \cdot \mathbf{w} = 0 \\ \int_K i\omega \underline{\underline{\sigma}}^K : \underline{\underline{\xi}} + \int_K \mathbf{v}^K \cdot \nabla \cdot (\underline{\underline{C}}^K \underline{\underline{\xi}}) - \int_{\partial K} \lambda^{\partial K} \cdot \underline{\underline{C}}_K \underline{\underline{\xi}} \cdot \mathbf{n} = 0 \\ \sum_{K \in \mathcal{T}_h} \int_{\partial K} (\underline{\underline{\sigma}}^K \cdot \mathbf{n}) \cdot \eta - \sum_{K \in \mathcal{T}_h} \int_{\partial K} \tau \mathbf{I} (\mathbf{v}^K - \lambda^{\partial K}) \cdot \eta = 0 \end{array} \right.$$

# Contents

2D Helmholtz elastic equations

Notations and definitions

Hybridizable Discontinuous Galerkin method

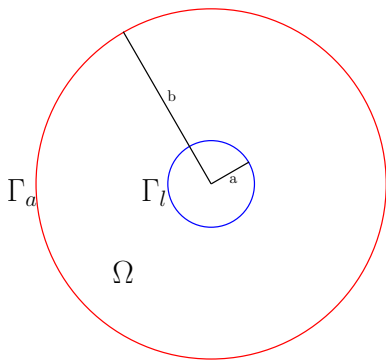
Numerical results

Disk-shaped scatterer problem

Marmousi test-case

Conclusions-Perspectives

# Disk-shaped scatterer problem



Computational domain  $\Omega$   
setting

- ▶  $a = 2000.0\text{m}$  and  $b = 8000.0\text{m}$
- ▶ Physical parameters in  $\Omega$  :
  - ▶  $\rho = 1\text{kg.m}^{-3}$
  - ▶  $\lambda = 8\text{GPa}$
  - ▶  $\mu = 4\text{GPa}$
- ▶  $\Gamma_l$  free surface boundary :  
 $\underline{\sigma}\mathbf{n} = 0$
- ▶  $\Gamma_a$  absorbing boundary :  
 $\underline{\underline{\sigma}}\mathbf{n} = \nu_p(\mathbf{v} \cdot \mathbf{n})\mathbf{n} + \nu_s(\mathbf{v} \cdot \mathbf{t})\mathbf{t}$
- ▶ Three meshes :
  - ▶ 1200 elements
  - ▶ 5400 elements
  - ▶ 22000 elements

# Disk-shaped scatterer problem

Elements	Order	CPU Time (s)			Memory (MB)		
		HDG	UDG	IPDG	HDG	UDG	IPDG
1200	2	0.7			32		
5100	2	3.0			161		
21000	2	14.0			728		
1200	3	1.7			57		
5100	3	7.6			283		
21000	3	34.8			1284		
1200	4	3.9			86		
5100	4	17.7			430		
21000	4	79.1			1953		

# Disk-shaped scatterer problem

Elements	Order	CPU Time (s)			Memory (MB)		
		HDG	UDG	IPDG	HDG	UDG	IPDG
1200	2	0.7	2.6	2.4	32	269	70
5100	2	3.0	15.0	11.9	161	1360	369
21000	2	14.0	94.8	58.0	728	6578	1857
1200	3	1.7	5.4	6.8	57	525	190
5100	3	7.6	38.8	35.9	283	2921	1017
21000	3	34.8	252.0	197.8	1284	14131	5126
1200	4	3.9	10.5	15.7	86	895	428
5100	4	17.7	67.0	87.9	430	4537	2279
21000	4	79.1	452.8	520.7	1953	21186	11503

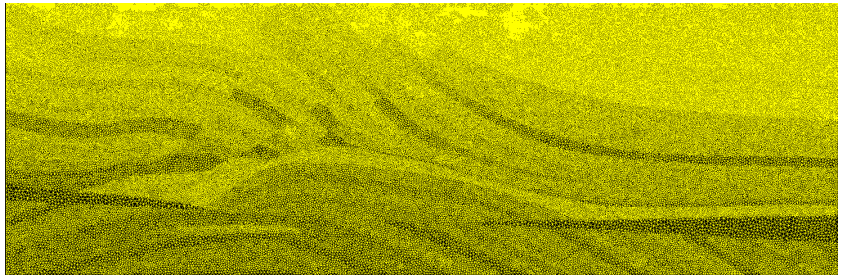
# Disk-shaped scatterer problem

Elements	Order	CPU Time			Memory		
		HDG	UDG	IPDG	HDG	UDG	IPDG
1200	2	1	3.7	3.4	1	8.4	2.2
5100	2	1	5.0	4.0	1	8.4	2.3
21000	2	1	6.8	4.1	1	9.0	2.6
1200	3	1	3.1	4.0	1	9.2	3.3
5100	3	1	5.1	4.7	1	10.3	3.6
21000	3	1	7.2	5.7	1	11.0	4.0
1200	4	1	2.7	4.0	1	10.4	5.0
5100	4	1	3.8	5.0	1	10.5	5.3
21000	4	1	5.7	6.6	1	10.8	5.9

# Disk-shaped scatterer problem

Elements	Order	CPU Time			Memory		
		HDG	UDG	IPDG	HDG	UDG	IPDG
1200	2	1	3.7	2.0	1	8.4	2.2
5100	2	1	5.0	2.5	1	8.4	2.3
21000	2	1	6.8	3.0	1	9.0	2.6
1200	3	1	3.1	1.8	1	9.2	3.3
5100	3	1	5.1	3.8	1	10.3	3.6
21000	3	1	7.2	3.0	1	11.0	4.0
1200	4	1	2.7	1.9	1	10.4	5.0
5100	4	1	3.8	2.7	1	10.5	5.3
21000	4	1	5.7	5.4	1	10.8	5.9

# Marmousi test-case



Computational domain  $\Omega$  composed of 235000 triangles

# Parallel results for the Marmousi test-case with the HDG-P2 scheme

	CPU Time construction (s)	CPU Time resolution. (s)	Maximum Memory (MB)
sequential	67	133	9927
2 proc. (2/1)	32	93	5892
4 proc. (2/2)	15	56	3340
8 proc. (4/2)	8	38	2092
16 proc. (4/4)	4	39	3695
32 proc. (4/8)	2	21	1312
64 proc. (8/8)	1	19	893

# Contents

2D Helmholtz elastic equations

Notations and definitions

Hybridizable Discontinuous Galerkin method

Numerical results

Conclusions-Perspectives

# Conclusions-Perspectives

## Conclusions

- ▶ The HDG scheme has the correct convergence order ( $p + 1$ )
- ▶ On a same mesh the HDG formulation is more competitive in terms of memory and computational time than the upwind flux DG formulation and the IPDG method

# Conclusions-Perspectives

## Conclusions

- ▶ The HDG scheme has the correct convergence order ( $p + 1$ )
- ▶ On a same mesh the HDG formulation is more competitive in terms of memory and computational time than the upwind flux DG formulation and the IPDG method

## Perspectives

- ▶ Develop 3D Upwind flux DG and HDG formulations for Helmholtz equations
- ▶ Solution strategy for the HDG linear system

Thank you !

